Comparison of VSC and Z-Source Converter: Power System Application Approach

Masoud Jokar KOUHANJANI, Ali Reza SEIFI

Department of Power and Control Engineering, School of Electrical and Computer Engineering, Shiraz University, Zand Street, Shiraz, Iran

masoudjokar@hotmail.com, seifi@shirazu.ac.ir

DOI: 10.15598/aeee.v15i1.1766

Abstract. *Application of equipment with power electronic converter interface such as distributed generation, FACTS and HVDC, is growing up intensively. On the other hand, various types of topologies have been proposed and each of them has some advantages. Therefore, appropriateness of each converter regarding to the application is a main question for designers and engineers. In this paper, a part of this challenge is responded by comparing a typical Voltage-Source Converter (VSC) and Z-Source Converter (ZSC), through high power electronic-based equipment used in power systems. Dynamic response, stability margin, Total Harmonic Distortion (THD) of grid current and fault tolerant are considered as assessment criteria. In order to meet this evaluation, dynamic models of two converters are presented, a proper control system is designed, a small signal stability method is applied and responses of converters to small and large perturbations are obtained and analysed by PSCAD/EMTDC.*

Keywords

Small signal analysis, state space model, Total Harmonic Distortion, Voltage-Source Converter, Z-Source Converter.

1. Introduction

Nowadays, applications of power electronic-based equipment are predominantly widespread from high power converter usage in power system such as Distributed Generation (DG), HVDC and FACTS, until electric machinery drive circuits and low power converters in communication industry. The chief parts of them are converters classified into two main categories relevant to high power applications in power system, according to terminal voltage and current waveforms at the DC port:

- Current-Source Converter (CSC) is a converter in which the DC-side current maintains the same polarity; therefore, the direction of power flow is adjusted by the DC-side voltage polarity.
- Voltage-Source Converter (VSC), in contrast, keeps the same voltage polarity. The direction of power flow is determined by the polarity of DC-side current.

The Z-Source Converter proposed by [1] has a specific characteristic that provides the capability to buck or boost the output voltage when in rectification or inversion mode. It has a valuable feature due to two particular ideas added to the basic VSC.

- Turning on at least one leg of switches set, a shoot-through mode, which is forbidden in conventional converters.
- X-shaped impedance network includes two pairs of capacitors and inductances, maintains energy in the shoot-through state.

As shown in Fig. 1(b), a typical ZSC includes an impedance network. Its duty is storing energy in the shoot-through state when all six switches are on. In the shoot-through state all three parts, impedance network DC and AC-sides, are isolated and the inductances of network are charged by capacitors. While the non-shoot-through state, the energy of DC-source is transferred to capacitors and the absorbed energy of inductances is delivered to AC-grid at the point of common coupling. The shoot-through state is implemented by turning on all the switches. It is forbidden in VSC, shown in Fig. 1(a), because the capacitor is a short circuit and discharged in switches, leading to intensive damage.

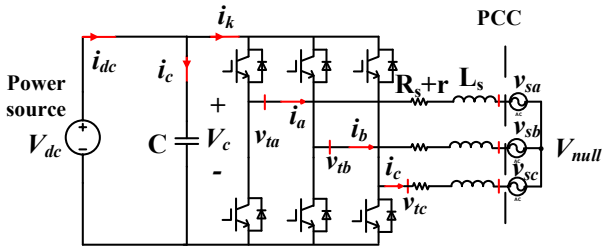

(a) Voltage-Source Converter.

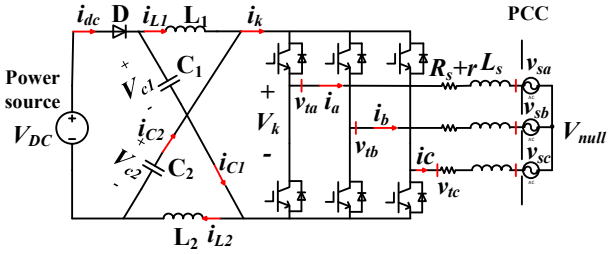

(b) Z-Source Converter.

Fig. 1: Circuit of 3-phase.

A lot of literature has been devoted to various usage of ZSC. There is a clear evidence of the ascendance in doing research on finding various suitable applications of ZSC For instance, distributed generation [2], [3], [4], [5], [6], [7], [8] and [9], uninterruptable power supply [10], electric vehicles [11] and [12] adjustable speed drive [13] and [14] and so on. A dynamic model that describes the behavior of VSC with appropriate DC-side voltage control and active and reactive power controllers are provided in [15]. In [16], [17] and [18] a dynamic model and a small signal model of Z-Source Converter are proposed; however, Z-Source Converter is considered as a basic DC/DC-power conversion application. Therefore, a section of this study is allocated to expand the proposed dynamic model to become appropriate for comprehensive assessment of its response.

In terms of comparison, a comprehensive work is done by [19]. It concludes that, ZSC has lower average switching device power and provides higher efficiencies in most operation ranges. Constant power ratio is raised over conventional PWM converter notably. Moreover, significant reliability development of ZSC is very important advantage. Due to the fact that ZSC has potential advantages in contrast with traditional converters, it is expected to be applied in vast range of power electronic-based equipment used in power system and motor drive circuits. In order to realize whether it is a suitable substitution for conventional converters in high power applications, this paper mainly allocated to compare dynamic responses of VSC and ZSC when they are encountered to changes of active and reactive demands of AC-side. Stability margin and THD which are other important criteria in power system point of view are taken into account and contribute to make the study more precise.

This paper is organized as follows. The mathematical models describing dynamic behaviour of VSC and ZSC are presented in Section 2. The comprehensive control system based on current control method which obtains AC-side currents and the voltage at PCC in rotary reference frame as input signals and deliver well-suited modulation signals to the converter are considered in Section 3. A comparison between VSC and ZSC regarding to stability and output harmonics of two converters is done in Section 4. Time domain results that illustrate the response of indicated converters to small and large changes in working point based on various scenarios are provided in Section 5. Conclusion commonly is delivered in Section 6.

2. Dynamic Model of VSC and ZSC

Figure 1 illustrates the generic electrical circuit model of typical VSC and ZSC. As illustrated, DC-circuit which can be DC-source of energy such as a renewable energy source or a part of DC-line is considered by constant DC-power supply that is also capable to absorb the energy in rectification mode of operation. In this paper, without loss of generality, some simplifications are assumed:

- Switching losses are neglected, resulting from both shoot-through and active states operation. Moreover, all switches are considered fast sufficient that has no time constant.
- Conduction loss which is a consequence of interior resistance of switches and passive components in impedance network is ignored. If more accuracy is desired, the converter losses can be represented by small resistance in series with R_s.

2.1. Voltage-Source Converter

The fundamental frequency component of terminal voltages for both converters in Fig. 1 is [17]:

$$v_t(t) = \frac{mV_{dc}(t)}{2}, \tag{1}$$

where $v_t(t)$ is the AC-terminal voltage and m is the converter modulation index which is M (arbitrary constant modulation index) for VSC and $M/(1-2d(t))$ for ZSC [1] and [17]. A dynamic model of AC-circuit in abc reference frame is [17]:

$$v_{tabc}(t) = L_s \frac{\mathrm{d}i_{sabc}}{\mathrm{d}t} + R_s i_{sabc} + v_{sabc}, \tag{2}$$

where $v_{sabc}(t) = [v_{sa}(t) \cdot v_{sb}(t) \cdot v_{sc}(t)]^T$ and $i_{sabc}(t) = [i_{sa}(t) \cdot i_{sb}(t) \cdot i_{sc}(t)]^T$. R_s and L_s are equivalent series resistance and inductance of the RL filter and transformer, between the converter terminal and PCC. By applying transformation matrix $\mathbf{K}_s$ [17] in Eq. (2), differential equations describing dynamic behavior of AC-circuit in dq reference frame are obtained as follows:

$$\frac{\mathrm{d}i_{sdq}(t)}{\mathrm{d}t} = \frac{R_s}{L_s} i_{sdq}(t) \pm \omega_e i_{sqd}(t) + \frac{1}{L_s}(v_{tdg}(t) - v_{sdq}(t)), \tag{3}$$

where $\theta = \int_0^t \omega_e(\zeta) + \theta_0$ and ω_e is the power system frequency. The angle is $\omega_e(t)$ provided by the Phase-Locked Loop (PLL), arbitrary assumed here to align system voltage with the d-axis leading to $v_{sq}(t) = 0$. The DC-voltage dynamic expression is deduced based on energy balance between the AC and DC-side of the converter.

$$V_c(t) i_{dc}(t) = p(t) - P_L(t), \tag{4}$$

where $p(t)$ is instantaneous real power at AC-terminal of converter which is defined in dq reference frame as [17]:

$$p(t) = \frac{3}{2}(v_{td}(t) i_{sd}(t) + v_{tq}(t) i_{sq}(t) + 2v_{t0}(t) i_{t0}(t). \tag{5}$$

It should be noted that the last term of Eq. (5) is omitted due to the fact that $i_{ta}(t) + i_{tb}(t) + i_{tc}(t) = 0$. $P_L(t)$ includes both conduction and switching losses that are ignored in this study based on [15].

In order to present all dynamic equations in the form of differential equations, capacitor voltage considered as a state variable and Eq. (5) is rewritten as:

$$\frac{\mathrm{d}V_c(t)}{\mathrm{d}t} = \frac{1}{CV_c(t)} \left(\frac{3}{2} \cdot (v_{td}(t) i_{sd}(t) + v_{tq}(t) i_{sq}(t)) \right) + \frac{i_{dc(t)}}{C}. \tag{6}$$

dq-frame components of converter terminal voltage, $v_{td}(t)$ and $v_{tq}(t)$, will be determined based on control system equations.

2.2. Z-Source Converter

As opposed to VSCs, Z-Source Converters have the shoot-through state, leading to different circuit topology from the non-shoot-through state illustrated in Fig. 1. Therefore, two operation modes in the switching period should be taken into account and average procedure will be held consequently. In mode 1, real energy transferred between AC and DC-sides; however, in mode 2, the path of transferring energy is blocked by diode D in DC-side and set of IGBTs in AC-side, so DC-power source, impedance network and AC-grid are decoupled as shown in Fig. 2. The duty ratio of switches, $d(t)$, which is generally not constant, is defined as the shoot-through duty ratio. Correspondingly, equation Eq. (3) is eligible for describing dynamic behavior of AC-circuit of ZSC; however, all terms should be multiplied to $1 - d(t)$, non-shoot through factor, in operation mode 1 and $d(t)$ for mode 2, distinctly. In order to decrease the number of equations, the impedance network is considered symmetric, which is $L_1 = L_2 = L$ and $C_1 = C_2 = C$.

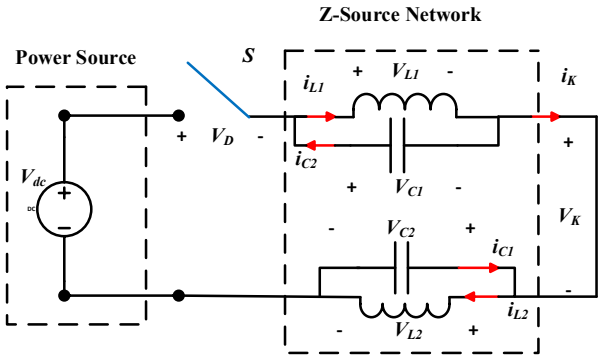

Fig. 2: ZSC in shoot through state.

$$(1 - d(t))L \cdot \frac{\mathrm{d}i_L(t)}{\mathrm{d}t} = = (V_{dc}(t) - V_c(t)) \cdot (1 - d(t)), \tag{7}$$

$$(1 - d(t))C \cdot \frac{\mathrm{d}V_c(t)}{\mathrm{d}t} = = (i_L(t) - i_k(t)) \cdot (1 - d(t)). \tag{8}$$

As shown in Fig. 2, DC-side equations for the shoot-through state are modified into:

$$d(t)L \cdot \frac{\mathrm{d}i_L(t)}{\mathrm{d}t} = V_c(t) d(t), \tag{9}$$

$$d(t)C \cdot \frac{\mathrm{d}V_c(t)}{d(t)} = -i_L(t) d(t). \tag{10}$$

So far, electrical circuits of VSC and ZSC are modeled in the form of differential equations. By averaging on a switching period, adding equations for shoot-through and non-shoot-through states, state space close form of equations is obtained completely.

3. Active and Reactive Power Controllers

The main purpose of the control system is to achieve appropriate output-active and output–reactive power

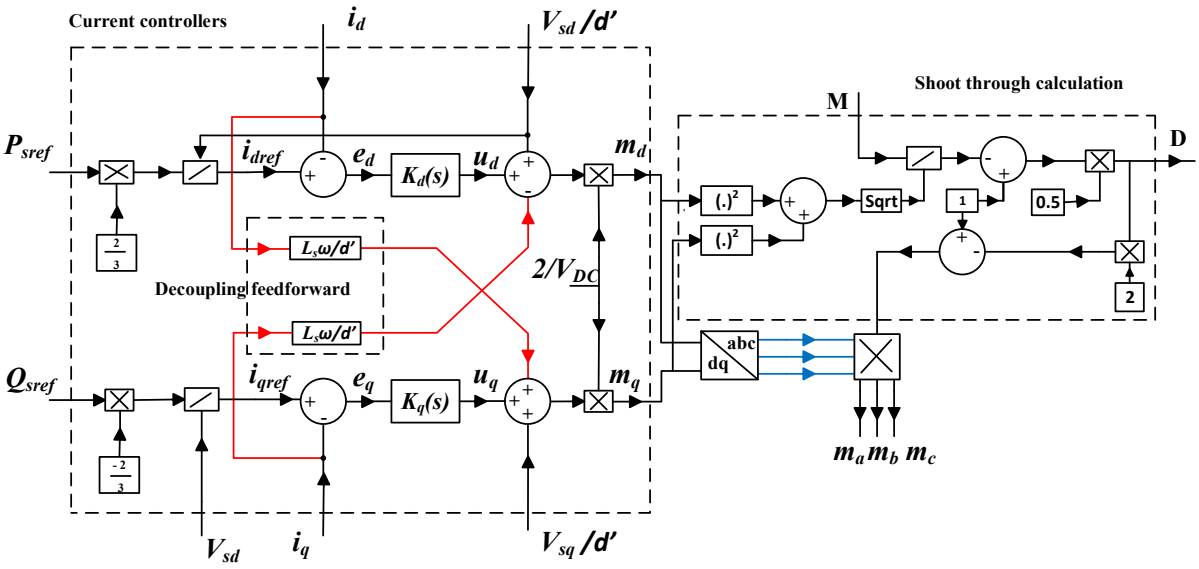

Fig. 3: Control system.

tracking exchanged with AC-grid at PCC. PI controller based on adjusting AC-current is taken into account for this work [15]. As illustrated in Fig. 3, active and reactive demand of AC-side are considered as reference input signals:

$$P_s(t) = \frac{3}{2} V_{sd}(t) i_d(t), \tag{11}$$

$$Q_s(t) = -\frac{3}{2} V_{sq}(t) i_d(t). \tag{12}$$

The reference value of dq-components of current, i_{dref} and i_{qref} can be obtained from a desired value of active and reactive powers by means of Eq. (11) and Eq. (12), respectively. A proportional-integral compensator in the form of $K(s) = k_p + \frac{k_i}{s}$ is sufficient for implementing the control process, due to the fact that all required signals are completely DC-quantities. The presence of $L_s\omega_e$ in Eq. (3) results in coupling two mentioned equations. Thus, $m_d(t)$ and $m_q(t)$ are identified as follows that are accomplished by cross coupling terms as shown in Fig. 3 so as to decouple remarked equations:

$$m_{dq}(t) = \frac{2\left(u_{dq}(t) + V_{sdq} \mp \dfrac{L_s\omega_e i_{qd}(t)}{d'}\right)}{V_{dc}(t)}, \tag{13}$$

where $u_d(t)$ and u_q are:

$$u_{dq}(t) = (k_p) + \frac{k_i}{p}(i_{dqref} - i_{dq}(t)), \tag{14}$$

$$\frac{\mathrm{d}z_{dq}(t)}{\mathrm{d}t} = i_{dqref} - i_{dq}(t). \tag{15}$$

The output signals of current controllers are dq-component of modulation signal, $m_d(t)$ and $m_q(t)$, which include only buck factor for VSC. In the other words, when they are transferred to abc-frame the amplitudes of sinusoidal signals are less than unity except in third harmonic injection condition [15]. However, by transforming modulation signals from dq-frame to abc-frame, the amplitude of AC-port voltage is acquired according to trigonometric equations:

$$\frac{M}{1-2d(t)} = \sqrt{m_d^2(t) + m_q^2(t)}. \tag{16}$$

On the other hand, similar abc-component of modulation signals could be more than one for ZSC, because of the fact that $m_d(t)$ and $m_q(t)$ contain buck and boost factors simultaneously. In addition, the function of current controllers is to find out appropriate value of shoot through $d(t)$ in order to provide desired value of instantaneous active and reactive powers. Therefore, shoot-through calculation box is added to control system that get buck index M as the arbitrary factor and produce suitable shoot through index. It should be noted that consequently the amplitude of abc-frame of modulation signals is equal to M. In order to complete dynamic formulations, dq-components of AC-terminal voltage are delivered based on the state variables and inputs:

$$v_{tdq}(t) = m_{dq}(t)\frac{V_{dc}(t)}{2}. \tag{17}$$

Finally, after mathematical calculations differential equations describing dynamic behavior of ZSC connected to AC-grid can be presented as follows:

$$\begin{aligned} L_s\frac{\mathrm{d}i_d(t)}{\mathrm{d}t} &= -(R_s + d'K_p)i_d(t) + \\ &+ d'K_i z_d(t) + d'I_{dref}K_p, \end{aligned} \tag{18}$$

$$L_s\frac{\mathrm{d}i_q(t)}{\mathrm{d}t} = -(R_s + d'K_p)i_q(t) + \\ +d'K_i z_q(t) + d'I_{qref}K_p, \tag{19}$$

$$L\frac{\mathrm{d}i_L(t)}{\mathrm{d}t} = (d-d)v_c(t) + d'V_{dc}(t) - R_L i_L(t), \tag{20}$$

$$C\frac{\mathrm{d}v_c(t)}{\mathrm{d}t} = (d'-d)i_L(t) - \frac{3d'(1-2d)}{2V_{dc}(t)}\cdot \\ \cdot\left[i_d(t)K_p(I_{dref}-i_d(t)) + i_d(t)z_d(t)K_i + \right. \\ +\frac{V_{sd}i_d(t)}{d'} + i_q(t)z_q(t)K_i + \\ \left.+i_q(t)K_q(I_{qref}-i_q(t))\right], \tag{21}$$

$$\frac{\mathrm{d}z_d(t)}{\mathrm{d}t} = I_{dref} - i_d(t), \tag{22}$$

$$\frac{\mathrm{d}z_q(t)}{\mathrm{d}t} = I_{qref} - i_q(t). \tag{23}$$

4. Stability and THD Comparison

In this section, a comparison between ZSC and conventional VSC according to first stability margin region and secondly harmonic of AC-terminal voltages are evaluated.

4.1. Small Signal Stability

The main method that attempts to identify stability of a nonlinear system like both ZSC and VSC directly is Lyapunov's method based on the sign of Lyapunov's function and its time derivative. However, the stability of a nonlinear system can also be given by the roots of characteristic equation of the system of first approximation obtained by linearizing equations around an equilibrium point [20].

The studied case is applied to analyze the stability of the converters after encountering small disturbances based on the parameters shown in Tab. 1. For improving dynamic response of the converters, selection of appropriate parameters of controllers can be done based on traces of eigenvalues. The eigenvalue spectrum of VSC is shown in Fig. 4 as a function of K_p and K_i respectively. It can be seen that increase of K_p causes oscillation reduction, however, after $K_p = 0.04$ the stability margin of the system is decreased due to real part reduction of eigenvalues. On the other hand, K_i increasing can improve stability, but after $K_i = 2$ all modes become oscillating. Similar study has been done for ZSC, however, in addition to controller's parameters the impact of impedance network components are taken into account. A base-case scenario and participation factors, indicating the relation between states and modes, are provided in Tab. 2.

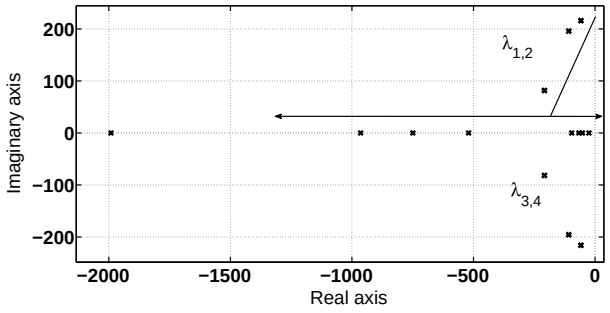

(a) Increase of k_p, $0.01 < k_p < 0.2$.

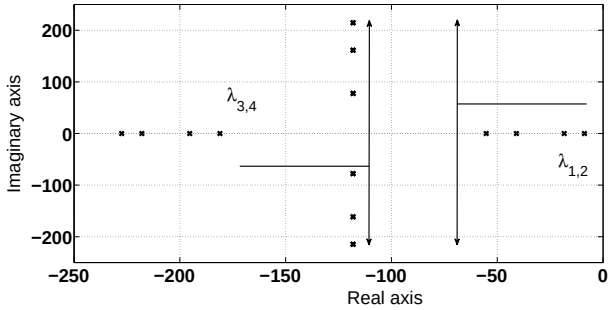

(b) Increase of k_i, $0.1 < k_i < 6$.

Fig. 4: Traces of VSC's eigenvalues for changes of controller's parameters.

Tab. 1: Parameters of case study.

Parameters	Value
Rated active power P_s	2.5 MW
Rated reactive power Q_s	1 MVar
AC system nominal voltage (L−L)	480 V
AC equivalent Inductance L_s	100 µH
AC equivalent Resistance R_s	1.63 mΩ
Nominal frequency	60 Hz
DC capacitance C	1000 µF
DC inductance L	1 mH
Nominal DC voltage V_{dc}	1250 V
Current controller K_p	0.05 Ω
Current controller K_i	5 Ω·s^{-1}
Carrier frequency	1.5 kHz

Tab. 2: Parameters of case study.

	$\lambda_{1,2} = -5 \pm j840$	$\lambda_{3,4} = -2017$	$\lambda_{5,6} = -22.8$
i_d	0	1.011	0.011
i_q	0	1.001	0.011
i_L	0.5	0	0
v_C	0.5	0	0
z_d	0	0.011	1.011
z_q	0	0.011	1.011

All participation factors are normalized into infinite norm. There are four evanescent modes and two oscillation modes. As shown in Tab. 2, $\lambda_{3,4}$ are highly sensitive to state variables i_d and i_q; therefore, they are chiefly under influence of k_p and k_i. Likewise, $\lambda_{5,6}$ are mainly affected by k_p and k_i. $\lambda_{1,2}$ are only sensitive to state variables i_L and v_C, so they are affected mostly by the value of impedance network elements. As

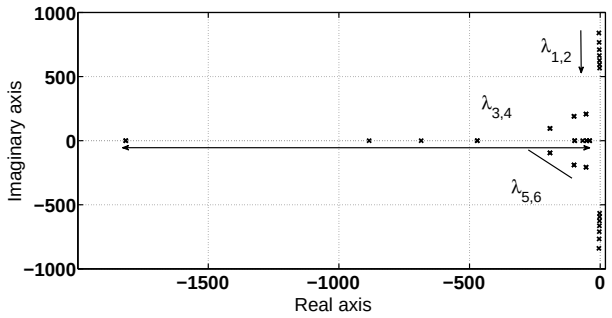

(a) Increase of k_p & L, $0.01 < k_p < 0.2$, 1 mH $< L <$ 2.2 mH.

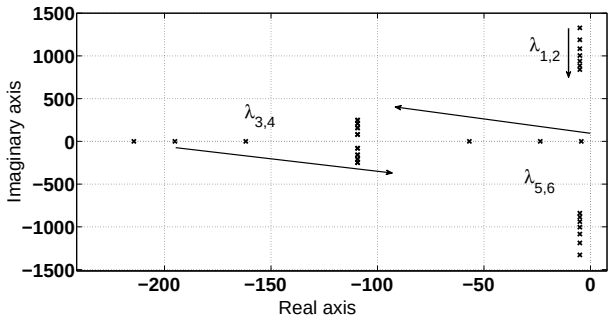

(b) Increase of k_i & C, $0.1 < k_i < 6$, 400 µF $< C <$ 1000 µF.

Fig. 5: Traces of ZSC's eigenvalues for changes of controllers' and impedance network's parameters individually.

predicted from participation factors and illustrated in Fig. 5, $\lambda_{1,2}$ is dependent on DC-side parameters, while controllers' parameters effects are restricted to eigenvalues related to AC-side states. In Fig. 5(a), traces of eigenvalues are sketched as a function of k_p and L individually. By increasing L, real part of $\lambda_{1,2}$ is decreased seldom; however, it causes stability margin reduction. But the imaginary part or oscillation reduction is significant, resulting from the fact that larger inductance is more reluctant against changes. It can be seen that as k_p is changed, only $\lambda_{3,4}$ and $\lambda_{5,6}$ are changed, when k_p is small they are conjugated eigenvalues, as k_p is increased, imaginary parts are decreased and they move toward stable region. Finally, they become four evanescent modes that two moves toward stable region and the other ones move toward instable region. Figure 5(b) shows the traces of eigenvalues as function of k_i and C.

Correspondingly, $\lambda_{1,2}$ are affected by C and the other eigenvalues are moved by k_i changing. The oscillation of $\lambda_{1,2}$ is reduced as C is increased. Although C is not in direct path of active power flow, at the early moments of changing the level of transferred energy, L is reluctant and C delivers a part of demanding energy. Therefore, larger capacitance leads to smaller oscillations. In contrast with the effect of k_p increasing, larger k_i can overall improve the disturbance suppression of AC-side dynamic response.

4.2. Total Harmonic Distortion

Both VSC and ZSC have an adverse relation between their output harmonics and the modulation index. In VSCs, modulation index is designed near 0.8 in order to improve the voltage profile during voltage sag occurrence. However for ZSCs, due to boosting capability, modulation index can be considered about 0.95. Therefore, ZSC potentially has lower THD. In spite of this, as shown in Fig. 6, the number of harmonics and THD are larger for VSC at the same modulation index, since impedance network prevents engendering subharmonics.

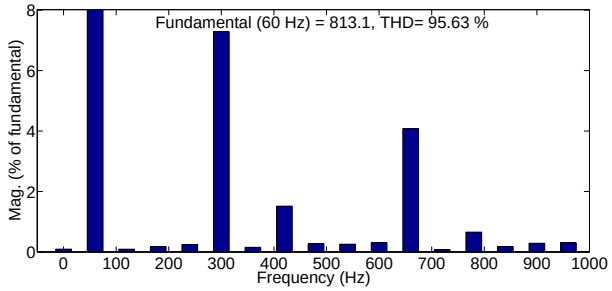

(a) VSC.

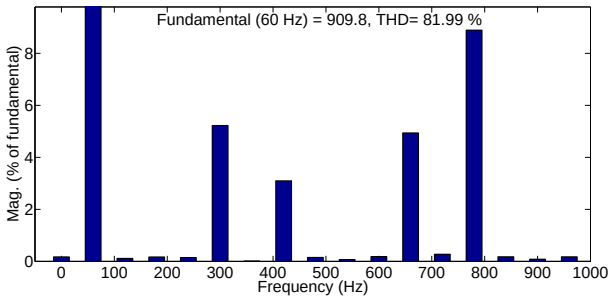

(b) ZSC.

Fig. 6: Total harmonic distortion.

5. Simulation and Results

A simulation model of Fig. 1 and controllers of Fig. 3 are implemented in PSCAD/EMTDC to verify the correctness of developed model of ZSC and accuracy of controllers, also compare the dynamic response and short current capacity of two converters. Small disturbance in active and reactive power demands for VSC are considered and the results are shown in Fig. 7.

As shown in Fig. 7, the active and reactive power signals are implemented at $t = 0.6$ s and $t = 1.1$ s, respectively in order to analyze the responses of converters more accurately. The ZSC is similarly encountered this scenario and results are shown in Fig. 8.

The proposed control system is working accurately and controlling the active and reactive power decou-

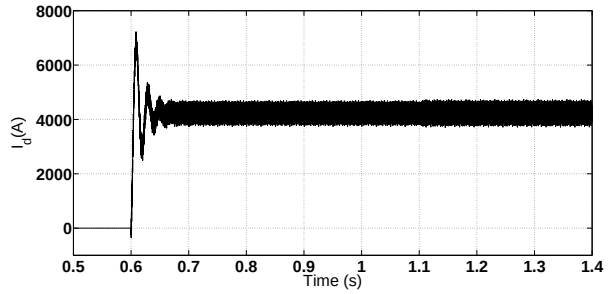

(a) I_d.

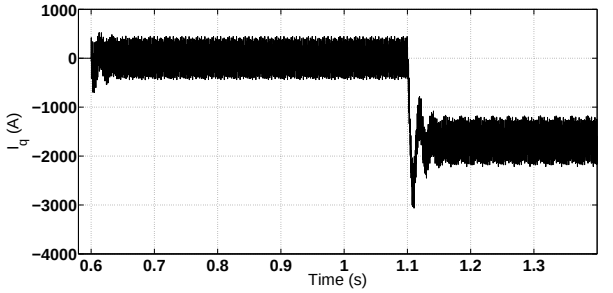

(b) I_q.

Fig. 7: Dynamic response of VSC to step change in active and reactive power.

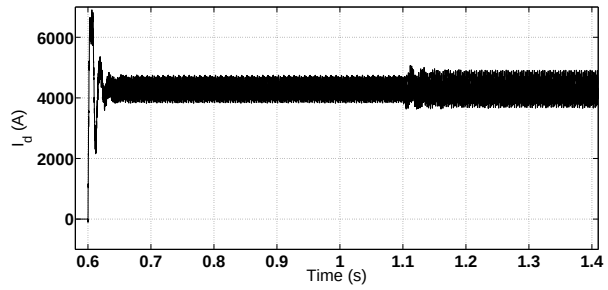

(a) I_d.

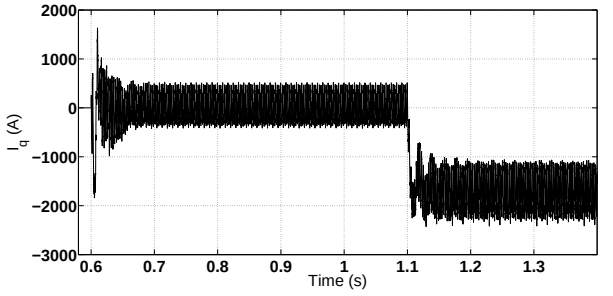

(b) I_q.

Fig. 8: Dynamic response of ZSC to step change in active and reactive power.

pled enough. It could be concluded from Fig. 7 and Fig. 8 that the control paths of I_d and I_q are separated for both converters. Because the active power changes have no effect on the value of reactive power and vice versa. By contrasting Fig. 7 and Fig. 8, ZSC has faster and smoother response to the reference signals; however, controller parameters are adjusted similarly. Presence of L in impedance network of ZSC justifies better response of I_d, since it resists versus rapid changes of energy by means of current. In another words, changing set point of active power by demand signal from the grid is realized by changing DC-current as DC-voltage is constant. For this purpose, DC-current should be passed through the inductances of impedance network which are reluctant against current changes.

Correspondingly, in Fig. 1(b), the voltage of capacitor is in relation with $V_k(t)$ accordingly reactive power demand of grid. Because the reactive power of grid could be adjusted by changing the amplitude of $v_t(t)$ that is in direct relation with $V_k(t)$ and $V_c(t)$. Its voltage is boosted during increment reactive power reference signal, so it allows increasing the voltage of AC-port. As a result, presence of C in the ZSC's circuit leads to better dynamic response of I_q than VSC one which is shown in Fig. 8(b).

In Fig. 9 a comparison according to fault tolerant criterion is held. ZSC restricts the fault current more than VSC, because of inductance L in the impedance network. As a result, this advantage leads to protecting accessories and switches.

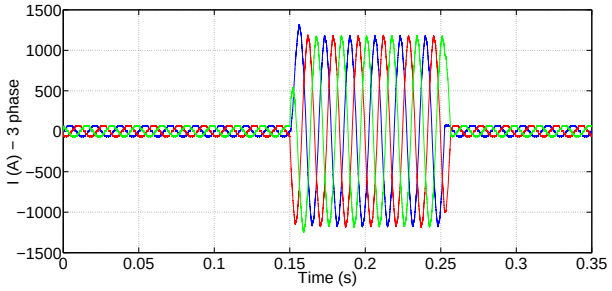

(a) VSC.

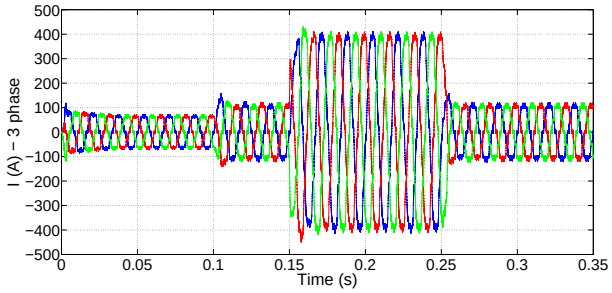

(b) ZSC.

Fig. 9: Three phase short circuit current.

6. Conclusion

In this paper, small signal model of a ZSC suitable for connecting to AC-grid is presented, and the effect of

each parameter on the behavior of the system is evaluated. In power electronic-based equipment such as DGs, dynamic response of the converter for frequency and voltage stability is definitely important. In addition to significant advantages of ZSC mentioned in previous works, it has also faster and smoother dynamic response, lower order of harmonics at AC-port and ability to limit the short circuit current in contrast with VSC that are significant criteria for designers and engineers in the process of selecting appropriate converter. The stability margin of this converter is fairly acceptable. Therefore, it could be a proper alternative for high power applications in near future.

References

[1] PENG, F. Z. Z-source inverter. *IEEE Transactions on Industry Applications*. 2003, vol. 39, iss. 2, pp. 504–510. ISSN 0093-9994. DOI: 10.1109/TIA.2003.808920.

[2] LI, Y., S. JIANG, J. G. CINTRON-RIVERA and F. Z. PENG. Modeling and Control of Quasi-Z-Source Inverter for Distributed Generation Applications. *IEEE Transactions on Industrial Electronics*. 2013, vol. 60, iss. 4, pp. 1532–1541. ISSN 0278-0046. DOI: 10.1109/TIE.2012.2213551.

[3] SIWAKOTI, Y. P. and G. E. TOWN. Performance of distributed DC power system using quasi Z-Source Inverter based DC/DC converters. In: *Twenty-Eighth Annual IEEE Applied Power Electronics Conference and Exposition (APEC)*. Orlando: IEEE, 2013, pp. 1946–1953. ISBN 978-147992407-3. DOI: 10.1109/APEC.2013.6520561.

[4] GE, B., H. ABU-RUB, F. Z. PENG, Q. LEI, A. T. DE ALMEIDA, F. J. T. E. FERREIRA, D. SUN and Y. LIU. An Energy-Stored Quasi-Z-Source Inverter for Application to Photovoltaic Power System. *IEEE Transactions on Industrial Electronics*. 2012, vol. 60, iss. 10, pp. 1532–1541. ISSN 0278-0046. DOI: 10.1109/TIE.2012.2217711.

[5] GAJANAYAKE, C. J., D. M. VILATHGAMUWA, P. C. LOH, R. TEODORESCO and F. BLAABJERG. Z-Source-Inverter-Based Flexible Distributed Generation System Solution for Grid Power Quality Improvement. *IEEE Transactions on Energy Conversion*. 2009, vol. 24, iss. 3, pp. 695–704. ISSN 1558-0059. DOI: 10.1109/TEC.2009.2025318.

[6] GAJANAYAKE, C. J., D. M. VILATHGAMUWA and P. C. LOH. Development of a Comprehensive Model and a Multiloop Controller for Z-Source Inverter DG Systems. *IEEE Transactions on Industrial Electronics*. 2007, vol. 54, iss. 4, pp. 2352–2359. ISSN 1557-9948. DOI: 10.1109/TIE.2007.894772.

[7] DEHGHAN, S. M., M. MOHAMADIAN and A. Y. VARJANI. A New Variable-Speed Wind Energy Conversion System Using Permanent-Magnet Synchronous Generator and Z-Source Inverter. *IEEE Transactions on Energy Conversion*. 2009, vol. 24, iss. 3, pp. 714–724. ISSN 1558-0059. DOI: 10.1109/TEC.2009.2016022.

[8] JUNG, J. W. and A. KEYHANI. Control of a Fuel Cell Based Z-Source Converter. *IEEE Transactions on Energy Conversion*. 2007, vol. 22, iss. 2, pp. 467–476. ISSN 1558-0059. DOI: 10.1109/TEC.2006.874232.

[9] TANG, Y., J. WEI and S. XIE. Grid-tied photovoltaic system with series Z-source inverter. *IET Renewable Power Generation*. 2013, vol. 7, iss. 3, pp. 275–283. ISSN 1752-1416. DOI: 10.1049/iet-rpg.2012.0335.

[10] HANIF, M., M. BASU and K. GAUGHAN. Understanding the operation of a Z-source inverter for photovoltaic application with a design example. *IET Power Electronics*. 2011, vol. 4, iss. 3, pp. 278–287. ISSN 1755-4535. DOI: 10.1049/iet-pel.2009.0176.

[11] ZHOU, Z. J., X. ZHANG, P. XU and W. X. SHEN. Single-Phase Uninterruptible Power Supply Based on Z-Source Inverter. *IEEE Transactions on Industrial Electronics*. 2008, vol. 55, iss. 8, pp. 2997–3004. ISSN 1557-9948. DOI: 10.1109/TIE.2008.924202.

[12] KULKA, A. and T. UNDELAND. Voltage harmonic control of Z-source inverter for UPS applications. In: *13th Power Electronics and Motion Control Conference (EPE-PEMC)*. Poznan: IEEE, 2008, pp. 657–662. ISBN 978-1-4244-1741-4. DOI: 10.1109/EPEPEMC.2008.4635339.

[13] GUO, F., L. FU, C.-H. LIN, C. LI, W. CHOI and J. WANG. Development of an 85-kW Bidirectional Quasi-Z-Source Inverter With DC-Link Feed-Forward Compensation for Electric Vehicle Applications. *IEEE Transactions on Power Electronics*. 2013, vol. 28, iss. 12, pp. 5477–5488. ISSN 1941-0107. DOI: 10.1109/TPEL.2012.2237523.

[14] PENG, F. Z., M. SHEN and K. HOLLAND. Application of Z-Source Inverter for Traction Drive of Fuel Cell-Battery Hybrid Electric Vehicles. *IEEE Transactions on Power Electronics*. 2007, vol. 22, iss. 3, pp. 1054–1061. ISSN 1941-0107. DOI: 10.1109/TPEL.2007.897123.

[15] PENG, F. Z., X. YUAN, X. FANG and Z. QIAN. Z-Source Inverter for Adjustable Speed Drives. *IEEE Power Electronics Letters*. 2003, vol. 99, iss. 2, pp. 33–35. ISSN 1540-7985. DOI: 10.1109/LPEL.2003.820935.

[16] PENG, F. Z., A. JOSEPH, J. WANG, M. SHEN, L. CHEN, Z. PAN, E. O. RIVERA and Y. HUANG. Z-source inverter for motor drives. *IEEE Transactions on Power Electronics*. 2005, vol. 20, iss. 4, pp. 857–863. ISSN 1941-0107. DOI: 10.1109/TPEL.2005.850938.

[17] YAZDANI, A. and R. IREVANI. *Voltage-Sourced Converters in Power Systems: Modeling, Control, and Applications*. 1st ed. New Jersey: Wiley, 2010. ISBN 978-0-470-52156-4. DOI: 10.1002/9780470551578.

[18] LIU, J., J. HU and L. XU. Dynamic Modeling and Analysis of Z Source Converter—Derivation of AC Small Signal Model and Design-Oriented Analysis. *IEEE Transactions on Power Electronics*. 2007, vol. 22, iss. 5, pp. 1786–1796. ISSN 1941-0107. DOI: 10.1109/TPEL.2007.904219.

[19] YU, K., F. L. LUO and M. ZHU. Voltage harmonic control of Z-source inverter for UPS applications. In: *5th IEEE Conference on Industrial Electronics and Applications (ICIEA)*. Taichung: IEEE, 2010, pp. 2169–2174. ISBN 978-1-4244-5046-6. DOI: 10.1109/ICIEA.2010.5515153.

[20] GAJANAYAKE, C. J., D. M. VILATHGAMUWA and P. C. LOH. Small-signal and signal-flow-graph modeling of switched Z-source impedance network. *IEEE Power Electronics Letters*. 2005, vol. 3, iss. 3, pp. 111–116. ISSN 1540-7985. DOI: 10.1109/LPEL.2005.859771.

[21] LOH, P. C., D. M. VILATHGAMUWA, C. J. GAJANAYAKE, Y. R. LIM and C. W. TEO. Transient Modeling and Analysis of Pulse-Width Modulated Z-Source Inverter. *IEEE Transactions on Power Electronics*. 2007, vol. 22, iss. 2, pp. 498–507. ISSN 1941-0107. DOI: 10.1109/TPEL.2006.889929.

[22] SHEN, M., A. JOSEPH, J. WANG, F. Z. PENG and D. J. ADAMS. Comparison of Traditional Inverters and Z-Source Inverter for Fuel Cell Vehicles. *IEEE Transactions on Power Electronics*. 2007, vol. 22, iss. 4, pp. 1453–1463. ISSN 1941-0107. DOI: 10.1109/TPEL.2007.900505.

[23] KUNDUR, P. *Power system stability and control*. 1st ed. New York: McGraw-Hill, 1994. ISBN 0-07-035958-X.

About Authors

Masoud Jokar KOUHANJANI was born in Shiraz, Iran. He received the B.Sc. degree in electrical engineering from Shiraz University of Technology, Shiraz, Iran, in 2011 and the M.Sc. degree in electrical engineering (power) from Shiraz University, Shiraz, Iran, in 2014. His research interests include power electronic interfaces, power system programing.

Ali Reza SEIFI was born in Shiraz, Iran. He received his B.Sc. in Electrical Engineering from Shiraz University, Shiraz, Iran, in 1991, his M.Sc. in Electrical Engineering from the University of Tabriz, Tabriz, Iran, in 1993 and his Ph.D. in Electrical Engineering from Tarbiat Modarres University (T.M.U.), Tehran, Iran, in 2001. He is currently the Professor in Department of Power and Control Engineering, School of Electrical and Computer Engineering, Shiraz University, Shiraz, Iran. His research interests include power plant simulations, power systems, electrical machine simulations, power electronics and fuzzy optimization.